

# Chapter 5

## Semiclassical $S$ -matrices

So far, this thesis has studied the quantum mechanics of Rydberg atoms in a time-independent external electromagnetic field. The preceding chapters have derived a fully quantum mechanical framework for calculating and interpreting the photoabsorption cross section of such an atom. The main tools in this framework are the scattering matrices  $\underline{S}^{\text{LR}}$  and  $\underline{S}^{\text{core}}$ , which describe the electron's motion in the long-range and core regions respectively. In the previous chapter, a method was described for calculating the long-range  $S$ -matrix for the case of an external magnetic field. These large scale quantum calculations yield an accurate  $S$ -matrix  $\underline{S}^{\text{LR}}(w)$  that can be studied using ideas from scaled variable recurrence spectroscopy. The Fourier transforms of the matrix elements  $S_{ll'}^{\text{LR}}(w)$  show sharp peaks in the scaled action domain, suggesting that certain quantum mechanical paths dominate the motion of the electron as it scatters off the long range potential.

As closed-orbit theory has shown [38, 37], the full interpretation of these quantum paths seen in the Fourier transform of  $\underline{S}^{\text{LR}}(w)$  emerges when semiclassical approximations are made in the long-range region. In this chapter I develop such an approximation for the long-range  $S$ -matrix. The main result, Eq (5.39), is a semiclassical formula for  $\underline{S}^{\text{LR}}$  that describes the motion of an atomic electron in an external magnetic field. My formula shows that, in the semiclassical limit,  $\underline{S}^{\text{LR}}$  can be constructed using the properties of the closed classical orbits of the electron. These closed orbits, which also appear in closed-orbit theory, are classical trajectories that are launched radially outward from a sphere in the matching region, scatter off the long range Coulomb and diamagnetic potentials and then return radially to the sphere.

Semiclassical scattering matrices have been used in other contexts previously. The idea of a semiclassical  $S$ -matrix originated with the work of Miller and coworkers in the 1970's [122]. In his approach, the  $S$ -matrix is written in terms of matrix elements of an energy-dependent Green's function. This theory has been used to treat a number of problems in molecular scattering theory [122]. These semiclassical ideas have been extended to atomic scattering problems, such as electron-hydrogen impact ionization [123], by Rost [124]. In a different field of physics, the ballistic conduction of electrons through quantum billiards has been studied using a semiclassical scattering matrix [125, 126, 127, 128, 129] alongside the Landauer formula [130] for the conductance. These diverse works share one thing in common: the semiclassical  $S$ -matrix is written in terms of a semiclassical Green's function.

My derivation of the semiclassical approximation to  $\underline{S}^{\text{LR}}$  follows this same route. First, the long-range  $S$ -matrix is written in terms of matrix elements of an energy dependent Green's function (Sec. 5.1). Then, after the semiclassical Green's function of Gutzwiller [22] has been introduced, the required matrix elements are calculated using the method of stationary phase (Sec. 5.2). This final step is both the most difficult and interesting one in the derivation. It is difficult because there are a number of assumptions needed to use the stationary phase technique - or at least the simple version of it - successfully. When these assumptions break down, the stationary phase integrals must be revisited with additional care. This is the case for the classical trajectory parallel to the magnetic field, for high angular momentum elements of  $\underline{S}^{\text{LR}}$ , and for bifurcations of closed orbits. In all of these cases, the general approach of using a semiclassical Green's function to extract the semiclassical  $S$ -matrix still applies. However, the naive stationary phase approximation for calculating the matrix elements of the Green's function must be modified. These special cases are treated in Sec. 5.3 and show the generality of the semiclassical approximation - when handled with care.

In spite of being subtle and difficult, the stationary phase integrals provide interesting information about the long-range  $S$ -matrix. Initially, the  $S$ -matrix is written as a sum over infinitely many classical trajectories that scatter off the long-range Coulomb and diamagnetic potentials. These infinitely many trajectories both leave and return to a sphere in the matching region with arbitrary values of the classical angular momentum  $p_\theta$ . The stationary phase integration essentially encodes the information about **all** of

these trajectories into a smaller subset of trajectories: the closed orbits that leave and return to the sphere with zero classical angular momentum ( $p_\theta = 0$ ). Thus, the stationary phase integrals place the closed orbits in a proper perspective. The closed orbits are **not** the only important trajectories for the long range  $S$ -matrix. Rather, the closed orbits are the orbits chosen to **represent** all others. This represents an important advance, as the closed orbits emerge rather mysteriously in standard closed-orbit theory.

It should be mentioned that, while closed-orbit theory contains the same closed orbits that will appear in the semiclassical  $S$ -matrix, a direct comparison with closed-orbit theory is difficult at this point. This is because closed-orbit theory only gives the photoabsorption cross section, whereas this chapter focuses on the the long-range  $S$ -matrix, which is not present in closed-orbit theory. Of course, the scattering matrices of this chapter can be used, along with the formula for the photoabsorption cross section to calculate the photoabsorption rate. This will be the topic of Ch. 6. Thus, I delay comparisons between my method and closed-orbit theory until then.

## 5.1 The $S$ -matrix and the Green's function: an exact relationship

The first step in deriving the semiclassical approximation to  $\underline{S}^{\text{LR}}$  is to relate this  $S$ -matrix to the energy dependent Green's function for the system [122]. In this section, I derive such a relationship between  $\underline{S}^{\text{LR}}$  and a Green's function obeying certain boundary conditions at a sphere ( $r = r_0$ ) in the matching region. To allow for the subsequent use of semiclassical approximations, the boundary conditions on the sphere will be chosen to coincide with those of the semiclassical Green's function.

The desired relationship between the Green's function and  $\underline{S}^{\text{LR}}$  can be derived by constructing the Green's function out of solutions of the homogeneous Schrödinger equation. This approach follows that of Ch. 3, where the outgoing-wave Green's function needed for the photoabsorption cross section was constructed. Because the techniques of Ch. 3 are used with little modification, the current derivation is presented in outline form only; more details of the method can be found in Ch. 3. The only difference in the current derivation is the boundary conditions imposed on the Green's function. For calculating  $\underline{S}^{\text{LR}}$  it is appropriate to impose traveling wave boundary conditions on the Green's function at a sphere

in the matching region ( $r = r_0$ ) that are consistent with the long-range  $S$ -matrix state of Ch. 2:

$$\underline{M}^{\text{LR}}(r) = \frac{1}{i\sqrt{2}} [\underline{f}^-(r)\underline{S}^{\text{LR}} - \underline{f}^+(r)]. \quad (5.1)$$

The multichannel  $S$ -matrix state, Eq. (5.1), can be incorporated into the Green's function once a channel expansion of the Green's function has been introduced:

$$G(\vec{x}, \vec{x}'; E) = \frac{1}{rr'} \sum_{i,j} \Phi_i(\Omega) \tilde{G}_{ij}(\vec{x}, \vec{x}'; E) \Phi_j^*(\Omega'), \quad (5.2)$$

$$\tilde{G}_{ij}(r, r'; E) = rr' \langle \Phi_i | G(\vec{x}, \vec{x}'; E) | \Phi_j \rangle. \quad (5.3)$$

As in Ch. 3, the multichannel Green's function  $\tilde{G}(r, r'; E)$  obeys the inhomogeneous differential equation, Eq. (3.13), is continuous at  $r = r'$ , and has a discontinuity in its first derivative at  $r = r'$  given by Eq. (3.17). The ansatz for the multichannel Green's function with the desired boundary conditions is given in terms of the long-range  $S$ -matrix state, Eq. (5.1):

$$\begin{aligned} \tilde{G}(r, r') &= [\underline{f}^-(r)\underline{S}^{\text{LR}} - \underline{f}^+(r)] \underline{A}(r') & r > r', \\ &= [-\underline{f}^-(r)\underline{S}^{\text{LR}}] \underline{B}(r') & r < r'. \end{aligned} \quad (5.4)$$

The conditions on the Green's function at  $r = r'$  give equations for the matrices  $\underline{A}(r')$  and  $\underline{B}(r')$ ,

$$(\underline{f}^- \underline{S}^{\text{LR}} - \underline{f}^+) \underline{A} + \underline{f}^- \underline{S}^{\text{LR}} \underline{B} = 0, \quad (5.5)$$

$$(\underline{f}^- \underline{S}^{\text{LR}} - \underline{f}^+) \underline{A} + \underline{f}^- \underline{S}^{\text{LR}} \underline{B} = 2, \quad (5.6)$$

which can be readily solved:

$$\underline{A}(r') = i\pi \underline{f}^-(r'), \quad (5.7)$$

$$\underline{B}(r') = -i\pi [\underline{f}^-(r') - \underline{S}^{\text{LR}\dagger} \underline{f}^+(r')]. \quad (5.8)$$

Because the  $S$ -matrix  $\underline{S}^{\text{LR}}$  describes electron flux being launched outward from a sphere in the matching region, the source radius  $r'$  will be fixed to the matching radius  $r_0$  and the observation radius  $r$  will be in the long range region so that  $r > r'$ . The relevant Green's function is obtained from Eqs. (5.4) and (5.7) and reads:

$$\tilde{G}(r, r_0) = i\pi [\underline{f}^-(r)\underline{S}^{\text{LR}} - \underline{f}^+(r)] \underline{f}^-(r_0). \quad (5.9)$$

Note that this form of the Green's function (5.9) is only valid in the matching region where the  $S$ -matrix state, Eq. (5.1), can be used.

The desired expression for the long-range  $S$ -matrix can be obtained by inverting Eq. (5.9) to find  $\underline{S}^{\text{LR}}$  in terms of the multichannel Green's function, Eq. (5.3). Two issues must be addressed before this step can be performed. First, the observation radius  $r$  must also be taken to the matching radius  $r_0$ , where the returning scattered wave will be observed (through the  $S$ -matrix elements). Second, the boundary conditions on the Green's function must be handled carefully. An inspection of Eq. (5.9) shows that the Green's function satisfies both incoming wave ( $-\underline{f}^+(r)$ ) and outgoing wave ( $\underline{f}^-(r)\underline{S}^{\text{LR}}$ ) boundary conditions in the observation coordinate  $r$ . The incoming wave term in Eq. (5.9) corresponds to electron flux traveling an infinitesimal distance from  $r_0$  to  $r$  (recall that the limit  $r \rightarrow r_0$  is also being taken) without scattering off the long-range region. The outgoing wave term in Eq. (5.9) corresponds to electron flux that travels outward into the long-range region where it then evolves in the long-range Coulomb and diamagnetic potential before being scattered back to the observation radius  $r \approx r_0$ . Clearly, because the long-range  $S$ -matrix describes this scattering process,  $\underline{S}^{\text{LR}}$  is related to the Green's function having **outgoing wave** boundary conditions on the sphere in the matching region. With this in mind, the outgoing wave part of Eq. (5.9) can be inverted to give an exact expression for the  $S$ -matrix, which is manifestly symmetric:

$$\underline{S}^{\text{LR}} = \frac{r_0^2}{i\pi} [\underline{f}^-(r_0)]^{-1} \underline{G}(r_0, r_0) [\underline{f}^-(r_0)]^{-1}. \quad (5.10)$$

It is critical to remember that the multichannel Green's-function matrix  $\underline{G}(r_0, r_0) = \tilde{\underline{G}}(r_0, r_0)/r_0^2$  in this equation obeys outgoing wave boundary conditions on the sphere at  $r_0$ . Equation (5.10) is an exact, general relationship valid for any atom and any configuration of external fields; all of the nontrivial physics is now encapsulated in the multichannel Green's function. In the absence of external fields, analytical expressions for this Green's function exist, and yield the expected long-range  $S$ -matrix  $e^{2i\beta}$  for the motion of an electron in a pure Coulomb potential.

One of the main advantages of the  $S$ -matrix formulation of the physics of the photoabsorption process now begins to emerge. The incoming wave boundary conditions of the Green's function in

Eq. (5.10) are precisely those obeyed by the semiclassical Green's function of van Vleck and Gutzwiller. Thus, the semiclassical Green's function can be used directly in Eq. (5.10) without modification, leading to an elegant method of deriving the semiclassical  $\underline{S}^{\text{LR}}$ . According to Eq. 5.10 the position space Green's function only needs to be projected onto the channel functions to find the  $S$ -matrix. The following section (Sec. 5.2) gives the semiclassical expression for the Green's function  $G(\vec{x}, \vec{x}'; E)$  and shows that this projection step can be carried out using stationary phase integration to obtain the multichannel Green's function  $\underline{G}(r_0, r_0)$  needed in Eq. (5.10).

## 5.2 Surface projections of the Green's function by the method of stationary phase

To derive the semiclassical  $\underline{S}^{\text{LR}}$ , the only remaining task is to introduce the semiclassical Green's function and project it onto the channel functions at a sphere in the matching region. If the required projection integrals are done numerically, this final step is fairly mundane, although very difficult. However, when the projection integrals are done, as in this section, by the method of stationary phase, this final step yields significant physical insight. The stationary phase treatment described below shows how certain classical orbits are selected over all others to encapsulate the contributions to the long-range  $S$ -matrix. In most cases, the significant orbits are the closed-orbits, which are launched from and return to the nucleus radially. I will call these classical orbits **radial trajectories** (also closed orbits). However, other nonradially launched orbits also contribute to the  $S$ -matrix. In some cases, such as near bifurcations or for high angular momenta element of the  $S$ -matrix, these nonradially launched orbits dominate over the radial ones.

A major advantage of the semiclassical  $S$ -matrix approach described in this chapter is that it enables a systematic exploration of the nonradial trajectories. In standard closed-orbit theory the emergence of the radial trajectories is somewhat obscured by the complicated formulas of the theory. Furthermore, this has made it difficult for researchers to extend closed-orbit theory to more accurately take the nonradial trajectories into account. The current section develops the basic tools used in performing the stationary phase integrals. The most elementary case is treated here: when the nonradial orbit do not

need to be **explicitly** included in the semiclassical  $S$ -matrix. However, the effects of the nonradial trajectories will be taken into account approximately when the Green's function is projected onto the channel functions. The more difficult cases, where the primitive stationary phase integrations fail, are presented in the following section.

While Eq. (5.10) is a general result, it is again useful to specialize to the case of a single channel atom in an external magnetic field along the  $z$ -axis. Then, the channel functions are simply the spherical harmonics, so that the projection integral needed to obtain  $\underline{G}(r_0, r_0)$  is:

$$G_{lm,l'm'}(E) = \int d\theta d\theta' d\phi d\phi' \sin\theta \sin\theta' Y_{lm}^*(\theta, \phi) G(\vec{x}, \vec{x}'; E) Y_{l'm'}(\theta', \phi'). \quad (5.11)$$

Because both the source and observation radii  $r$  and  $r'$  are fixed to the matching radius  $r_0$ , the explicit radial dependence of the Green's function is omitted in the following pages. A more convenient form of the projection integral, Eq. (5.11), is obtained by separating the integrals over  $\theta$  and  $\theta'$ ,

$$G_{lm,l'm'}(E) = \int d\theta d\theta' \sin\theta \sin\theta' Y_{lm}^*(\theta, \phi) G_{m,m'}(\theta, \theta'; E) Y_{l'm'}(\theta', \phi'), \quad (5.12)$$

from the integrals over  $\phi$  and  $\phi'$ ,

$$G_{m,m'}(\theta, \theta'; E) = \int d\phi d\phi' e^{-im\phi} G(\theta, \phi, \theta', \phi'; E) e^{im'\phi'}. \quad (5.13)$$

Now the issue of symmetry must be addressed. The general approach in this section will be to perform the integrals of Eqs. (5.12) and (5.13) using the method of stationary phase. The success of this method depends critically on the existence of well-isolated stationary phase points in the angles  $(\theta, \phi, \theta', \phi')$ . If continuous families of stationary phase points exist, the stationary phase approximation will fail. This occurs when there is a continuous symmetry that leaves the long-range Hamiltonian invariant. For the case of an atomic electron in an external magnetic field, there is one such continuous symmetry: rotation about the  $z$ -axis, which is often called azimuthal symmetry. This symmetry results in the Green's function being diagonal in the corresponding quantum number  $m$ . Because the stationary phase technique for the  $(\phi, \phi')$  integrals (5.13) fails for this case, these integrals must be done exactly. Note that when there are no symmetries in the Hamiltonian, as in the case of a Rydberg electron in crossed electric and magnetic fields, this complication is not present and all of the projection integrals in

Eqs. (5.12) and (5.13) can be done using the stationary phase approach. Given the recent experiments on hydrogen in perpendicular magnetic and electric fields, this would be an interesting case to investigate but it is not pursued here.

When the azimuthal symmetry is present, the integrals over  $(\phi, \phi')$  can be done analytically by using separation of variables on the full three dimensional Green's function  $G(\vec{x}, \vec{x}'; E)$ . Alternative, semiclassical approaches for handling continuous symmetries in the Green's function and in trace formulas have been given by Magner *et al.* [131] and by Creagh and Littlejohn [132, 133] respectively. Because these semiclassical methods are needlessly complicated and often subtle, I follow Delos and coworkers [38] and Bogomolny [36] in using separation of variables. The axial symmetry of a Rydberg electron in an external magnetic field is handled easily with the following ansatz for the Green's function in cylindrical coordinates  $(\rho, z, \phi)$ :

$$G(\vec{x}, \vec{x}') = \frac{1}{2\pi\sqrt{\rho\rho'}} \sum_m e^{im(\phi-\phi')} G_m(\rho, z, \rho', z'), \quad (5.14)$$

Then, the integrals over  $(\phi, \phi')$  in Eq. (5.13) can be done analytically:

$$G_{m,m'}(\theta, \theta') = \delta_{mm'} \frac{2\pi}{\sqrt{\rho\rho'}} G_m(\rho, z, \rho', z'). \quad (5.15)$$

As expected, the symmetry reduced Green's function, Eqs. (5.13) and (5.15), is diagonal in the azimuthal quantum number  $m$ . The factor  $1/\sqrt{\rho\rho'}$  is used in Eq. (5.14) to eliminate the first derivatives  $(\partial/\partial\rho)$  in the inhomogeneous equation for  $G_m(\rho, z, \rho', z')$ , which reads:

$$\left( \frac{1}{2} \frac{\partial^2}{\partial\rho^2} + \frac{1}{2} \frac{\partial^2}{\partial z^2} - \frac{m^2 - 1/4}{2\rho^2} + E - V(\rho, z) \right) G_m(\rho, z, \rho', z') = \delta(\rho - \rho') \delta(z - z'). \quad (5.16)$$

Finally, semiclassical approximations for the remaining nonintegrable motion in the Cartesian-like coordinates  $(\rho, z)$  can be made. The two-dimensional semiclassical Green's function of Guztwiller [18, 19, 20, 21] applies directly to Eq. (5.16):

$$G_m(\rho, z, \rho', z'; E) \approx \sum_{\text{class.traj.}} \frac{2\pi}{(2\pi i)^{3/2}} \sqrt{\left| \det \frac{\partial(p'_\rho, p'_z, t)}{\partial(\rho, z, E)} \right|} \exp\left(iS(\rho, z, \rho', z') - i\frac{\mu\pi}{2}\right). \quad (5.17)$$

Here, the sum includes all two-dimensional classical trajectories that propagate from  $(\rho', z')$  to  $(\rho, z)$  under the dynamics of the Langer-corrected [83] classical Hamiltonian  $H = p_\rho^2/2 + p_z^2/2 + m^2/2\rho^2 +$

$V(\rho, z)$ . The classical action associated with a particular trajectory is given as the integral,

$$S(\rho, z, \rho', z') = \int_{(\rho', z')}^{(\rho, z)} (p''_\rho d\rho'' + p''_z dz''). \quad (5.18)$$

The Maslov index  $\mu$  [24] is related to the topology of each orbit and is given by the number of sign changes in the determinant in Eq. (5.17) along each orbit. Furthermore, this determinant in Eq. (5.17) provides a measure of the stability of each orbit. More details about this determinant can be found in Appendix C.

When the semiclassical Green's function, Eq. (5.17) is inserted into Eq. (5.15), a semiclassical approximation to the symmetry-reduced Green's function is obtained:

$$G_{mm'}(\theta, \theta') = \delta_{mm'} \sqrt{2\pi} \sum_{\text{traj}} \frac{1}{r_0^2 |\dot{r}|} \frac{1}{\sqrt{\sin \theta \sin \theta'}} \sqrt{|A_1|} \exp \left( iS(\theta, \theta') - i\frac{\mu\pi}{2} - i\frac{3\pi}{4} \right), \quad (5.19)$$

where the classical stability  $A_1$  is the partial derivative:

$$A_1 = \left. \frac{\partial p'_\theta}{\partial \theta} \right|_{\theta'}. \quad (5.20)$$

According to Eq. (5.12), projecting the polar angle dependence  $(\theta, \theta')$  of this Green's function, Eq. (5.19), onto the spherical harmonics  $(Y_{lm}^*(\theta, 0), Y_{l'm'}(\theta', 0))$  gives the multichannel Green's function matrix  $G_{lm, l'm'}(E)$  (5.12) needed for the long-range  $S$ -matrix (5.10). In the following subsections, these projection integrals are done using the method of stationary phase. For this part of the derivation it is convenient to combine Eqs. (5.19) and (5.12) and write the result in the form:

$$G_{lm, l'm'}(E) = \sum_{\text{traj}} \int d\theta d\theta' \Lambda_{ll'}(\theta, \theta') \sqrt{|A_1(\theta, \theta')|} e^{i(S(\theta, \theta') - \mu(\pi/2))}, \quad (5.21)$$

$$\Lambda_{ll'}(\theta, \theta') = \frac{\sqrt{2\pi \sin \theta \sin \theta'}}{r_0^2 |\dot{r}|} e^{-i(3\pi/4)} Y_{lm}^*(\theta, 0), Y_{l'm'}(\theta', 0). \quad (5.22)$$

This shows that the multichannel Green's function needed for the long-range  $S$ -matrix (5.10), can be constructed by considering all of the classical trajectories that are fired outward from the point  $(r_0, \theta')$ , scatter off the long-range Coulomb and magnetic fields, and then return to the point  $(r_0, \theta)$  with a classical action  $S(\theta, \theta')$ . The contributions of these trajectories are integrated over the surface of the sphere  $r = r_0$  with the phase  $e^{iS(\theta, \theta')}$  and the angular factor  $\Lambda_{ll'}(\theta, \theta')$  to determine the Green's function. At

this point, these classical trajectories are not only the radially launched and returning closed-orbits. In Eq. (5.21), all classical orbits at energy  $E$ , even those launched nonradially from the matching sphere, must be included to calculate the semiclassical Green's function and thus the  $S$ -matrix  $\underline{S}^{\text{LR}}$ .

Equations (5.21) and (5.22) for the semiclassical Green's function  $\underline{G}(r_0, r_0; E)$  and Eq. (5.10) for the long-range  $S$ -matrix  $\underline{S}^{\text{LR}}$  represent a halfway point in the derivation for the semiclassical formula for  $\underline{S}^{\text{LR}}$ . It is interesting to note, that in their current form, these formulas show no artificial divergences at the points where new classical orbits bifurcate. Thus, they provide a useful starting point in treating various scenarios found in the physics of a Rydberg electron in an external magnetic field. In the remainder of this section, the elementary case of well-isolated classical orbits and low angular momenta ( $l, l'$ ) is studied.

### 5.2.1 Initial angle projection

The method of stationary phase integration is one of the most useful tools in semiclassical physics. This was first seen in Gutzwiller's derivation of the trace formula for the density of states [20]. In his work, the periodic orbits emerge as the stationary phase points of an integrand when the trace of the semiclassical Green's function, Eq. (5.17), is taken using the stationary phase technique. A similar idea will be seen in the projection of the semiclassical Green's function onto the spherical harmonics (5.21). Here, as in the trace formula, the dominant classical orbits - the closed orbits - appear when integrals of the semiclassical Green's function (the projection integrals) are evaluated using the method of stationary phase.

I now assume that the classical orbits contributing to the Green's function, Eq. (5.21), are well isolated. Then the classical action  $S(\theta, \theta')$  can be expanded in a Taylor series about the stationary phase points in the initial angle  $\theta' = \theta_i$ :

$$S(\theta, \theta') = S(\theta, \theta_i) + (\theta' - \theta_i) \frac{\partial S}{\partial \theta'} + \frac{1}{2} (\theta' - \theta_i)^2 \frac{\partial^2 S}{\partial \theta'^2}, \quad (5.23)$$

where the stationary phase points  $\theta_i$  are defined by the vanishing of the linear term in this expansion:

$$\frac{\partial S}{\partial \theta'} = -p'_\theta(\theta_i) = 0. \quad (5.24)$$

Immediately, it is seen that the stationary phase points correspond to classical trajectories that are launched radially ( $p_{\theta'} = 0$ ) outward from  $r_0$ . When a strong external magnetic field is applied to an atom, even a one-electron atom, the classical dynamics becomes chaotic, and there are infinitely many of these stationary phase points. In the end, each stationary phase point will contribute a term to the Green's function (5.21) and to the long-range  $S$ -matrix (5.10).

This analysis of the stationary phase points is valid when the other angular factors ( $\Lambda_{l'l'}(\theta, \theta')$  and  $A_1(\theta, \theta')$ ) in the integrand of Eq. (5.21) vary slowly compared to the classical action  $S(\theta, \theta')$ . This is true for low angular momentum elements of the Green's function  $G_{lm, l'm'}(E)$ , where the spherical harmonics in  $\Lambda_{l'l'}(\theta, \theta')$ , Eq. (5.22), oscillate slowly. For high angular momenta, these spherical harmonics oscillate rapidly and their variation must be taken into account. The required modifications for higher angular momentum will be developed in the next section (Sec. 5.3). However, for now it is assumed that the spherical harmonics, and consequently the matrix  $\Lambda_{l'l'}(\theta, \theta')$  vary slowly with the polar angles  $(\theta, \theta')$ .

Within the aforementioned approximations, the angular factor  $\Lambda_{l'l'}(\theta, \theta')$  and the amplitude  $A_1(\theta, \theta')$  are evaluated at the stationary phase point  $\theta' = \theta_i$  and pulled outside the integral over  $\theta'$  in the Green's function, Eq. (5.21):

$$G_{lm, l'm'}(E) = \sum_{\text{traj}} \int d\theta \Lambda_{l'l'}(\theta, \theta_i) \sqrt{|A_1(\theta, \theta_i)|} e^{i(S(\theta, \theta_i) - \mu\pi/2)} \times I_1. \quad (5.25)$$

The remaining integral  $I_1$  over the initial angle  $\theta'$  takes the form:

$$I_1 = \int d\theta' \exp\left(\frac{i}{2}(\theta' - \theta_i)^2 \frac{\partial^2 S}{\partial \theta'^2}\right). \quad (5.26)$$

In the stationary phase approach, the limits of this integrand are extended to  $\pm\infty$ , so that the integral can be done using the formula [24]:

$$\int_{-\infty}^{\infty} dx \exp\left(\frac{i}{2}x^2 \alpha\right) = \sqrt{\frac{2\pi i}{\alpha}}. \quad (5.27)$$

As Gutzwiller first showed, sign changes of amplitudes such as  $\frac{\partial^2 S}{\partial \theta'^2}$  along each classical trajectory must be taken into account when integrals such as Eq. (5.26) are performed. Labeling the number of sign changes of  $\frac{\partial^2 S}{\partial \theta'^2}$  along the classical orbit by the integer  $\nu$ , and performing the integral  $I_1$  using the general

formula, Eq. (5.27), one obtains:

$$I_1 = \sqrt{2\pi i} \left| \det \frac{\partial^2 S}{\partial \theta'^2} \right|^{-1/2} e^{-i\nu\pi/2}. \quad (5.28)$$

Using this result for  $I_1$  in Eq. (5.25), the channel space Green's function becomes,

$$G_{lm,l'm'}(E) = \sqrt{2\pi i} \sum_{\text{traj}} \int d\theta \Lambda_{ll'}(\theta, \theta_i) \sqrt{|A_2(\theta, \theta_i)|} e^{i(S(\theta, \theta_i) - \mu\pi/2)}, \quad (5.29)$$

where the overall amplitude  $A_2$  is the simple product:

$$A_2 = A_1 \left( \frac{\partial^2 S}{\partial \theta'^2} \right)^{-1} = - \frac{\partial p'_\theta}{\partial \theta} \Big|_{\theta'} \frac{\partial p'_\theta}{\partial \theta'} \Big|_{\theta}^{-1} = \frac{\partial \theta'}{\partial \theta} \Big|_{p'_\theta}. \quad (5.30)$$

The careful reader will notice that the index  $\nu$ , which counts the number of sign changes in the amplitude  $\frac{\partial^2 S}{\partial \theta'^2}$  along the classical orbit, has disappeared from the Green's function, Eq. (5.29); only the Maslov index  $\mu$  appears. As a convention, I will always absorb phases such as  $\nu$  that are generated in stationary phase integrals into the Maslov index  $\mu$  for the Green's function. With this convention, the index  $\mu$  of the Green's function is contextual: it always counts the composite number of sign changes of the amplitude whose square root currently appears in the Green's function. For example, when the classical amplitude of the Green's function is  $\sqrt{|A_1|}$  the index  $\mu$  counts the sign changes of  $A_1$ .

In this subsection, I have given the details of how the initial angle dependence of the Green's function can be projected out using the method of stationary phase integration. Because this approach will be used repeatedly in this thesis, the discussion has been lengthy. The resulting Green's function, Eq. (5.29), is written as a sum over classical trajectories that are launched radially ( $p'_\theta = 0$ ) from a sphere  $r = r_0$  in the matching region, but return to the sphere at a final polar angle  $\theta$  with any value of the classical angular momentum  $p_\theta$ . However, Eq. (5.29) specifies that this final angle dependence should also be projected onto the spherical harmonic  $Y_{lm}(\theta, 0)$  (contained in the factor  $\Lambda_{ll'}$ ).

### 5.2.2 Final angle projection

The final angle projection integral required by Eq. (5.29) for the Green's function  $G_{lm,l'm'}(E)$  is performed using the same stationary phase approach described above. First, the classical action  $S(\theta, p'_\theta)$

is expanded about the stationary phase point in the final polar angle  $\theta = \theta_f$ :

$$S(\theta, p'_\theta) = S(\theta_f, p'_\theta) + (\theta - \theta_f) \left. \frac{\partial S}{\partial \theta} \right|_{p'_\theta} + \frac{1}{2} (\theta - \theta_f)^2 \left. \frac{\partial^2 S}{\partial \theta^2} \right|_{p'_\theta}. \quad (5.31)$$

It is critical to note that the classical action is now a function of the initial angular momentum  $p'_\theta$  rather than the initial polar angle  $\theta'$  at the stationary phase points. This switch from  $\theta'$  to  $p'_\theta$  in the classical action is necessary as the initial angle dependence  $\theta'$  has been projected out of the Green's function, Eq. (5.29), and thus the classical action, already. However, as before, the stationary phase points of the action, Eq. (5.31), are the classical trajectories that travel radially as they return to  $r = r_0$ :

$$\left. \frac{\partial S}{\partial \theta} \right|_{p'_\theta} = p_\theta(\theta_f) = 0. \quad (5.32)$$

Again, assuming that the angular factors  $(\Lambda_{ll'}(\theta, \theta_i) \sqrt{|A_2(\theta, \theta_i)|})$  in Eq. (5.29) vary slowly with the final angle  $\theta$ , they can be evaluated at the stationary phase points  $\theta_f$  of the integrand. Using the expansion of the classical action, Eq. (5.31), in the Green's function, Eq. (5.29), gives the result:

$$G_{lm, l'm'}(E) = \sqrt{2\pi i} \sum_{\text{traj}} \Lambda_{ll'}(\theta_f, \theta_i) \sqrt{|A_2(\theta_f, \theta_i)|} e^{i(S(\theta_f, \theta_i) - \mu\pi/2)} \times I_2. \quad (5.33)$$

The integral  $I_2$ ,

$$I_2 = \int d\theta' \exp \left( \frac{i}{2} (\theta - \theta_f)^2 \left. \frac{\partial^2 S}{\partial \theta^2} \right|_{p_{\theta_i}} \right) = \sqrt{2\pi i} \left. \frac{\partial^2 S}{\partial \theta^2} \right|_{p'_\theta}^{-1/2} e^{-i\nu\pi/2}, \quad (5.34)$$

can be done using the formula, Eq. (5.27), as long as the sign changes in the amplitude  $\left. \frac{\partial^2 S}{\partial \theta^2} \right|_{p'_\theta}$  are kept track of in the index  $\nu$ .

The final form of the semiclassical approximation to  $G_{lm, l'm'}(E)$  is found by inserting Eq. (5.33) into Eq. (5.34):

$$G_{lm, l'm'}(E) = 2\pi i \sum_{\text{traj}} \Lambda_{ll'}(\theta_f, \theta_i) \sqrt{|A(\theta_f, \theta_i)|} e^{i(S(\theta_f, \theta_i) - \mu\pi/2)}. \quad (5.35)$$

Again, the index  $\nu$  has been absorbed into the Maslov index  $\mu$  of the Green's function that now tracks the sign changes of the overall amplitude  $A$  (rather than  $A_1$  or  $A_2$ ):

$$A = A_2 \left( \left. \frac{\partial^2 S}{\partial \theta^2} \right|_{p_{\theta_i}} \right)^{-1} = \left. \frac{\partial \theta'}{\partial \theta} \right|_{p_{\theta_i}} \left. \frac{\partial p_\theta}{\partial \theta} \right|_{p_{\theta_i}}^{-1} = \left. \frac{\partial \theta'}{\partial p_\theta} \right|_{p_{\theta_i}}. \quad (5.36)$$

This final amplitude  $A$  is a simple one dimensional derivative that can be calculated numerically for each classical trajectory without difficulty. Finally, the semiclassical approximation to  $\underline{S}^{\text{LR}}$  can be written down, using the semiclassical Green's function matrix derived in this section, Eq. (5.35), and the definition of the angular factor  $\Lambda_{l'l'}(\theta, \theta')$ , Eq. (5.22). The result,

$$S_{l'l',m}^{\text{LR}} = 2^{3/2}\pi^{1/2} \sum_{\text{c.o.}} \frac{1}{|\dot{r}|} \sqrt{|A| \sin \theta_i \sin \theta_f} \frac{Y_{lm}^*(\theta_f, 0) Y_{l'm}(\theta_i, 0)}{f_l^-(r_0) f_{l'}^-(r_0)} \exp \left( iS(\theta_f, \theta_i) - i\mu \frac{\pi}{2} - i \frac{3\pi}{4} \right), \quad (5.37)$$

is a sum over the closed orbits that are launched radially outward from the point  $(r_0, \theta_i)$  in the matching region, scatter classically off the long range Coulomb and magnetic field and then return to the point  $(r_0, \theta_f)$  again traveling radially.

One further approximation gives the semiclassical  $\underline{S}^{\text{LR}}$  that will be used in subsequent numerical calculations. For highly excited electrons with small matching radii  $r_0$  and low orbital angular momenta it is appropriate to use the asymptotic, zero-energy forms of the Coulomb functions in Eq. (5.37). The required formulas can be found in Ch. 2, Eqs. (2.4) and (2.5), and yield:

$$\frac{1}{|\dot{r}| f_l^-(r_0) f_{l'}^-(r_0)} \rightarrow -i\pi (-1)^{l+l'} e^{2i\sqrt{8r_0}}, \quad (5.38)$$

in which case the long-range  $S$ -matrix reads:

$$S_{l'l',m}^{\text{LR}}(E, B) = (2\pi)^{3/2} (-1)^{l+l'} \sum_{\text{c.o.}} \sqrt{|A| \sin \theta_i \sin \theta_f} Y_{lm}^*(\theta_f, 0) Y_{l'm}(\theta_i, 0) \times \exp \left( iS + 2\sqrt{8r_0} - i\mu \frac{\pi}{2} + i \frac{3\pi}{4} \right). \quad (5.39)$$

In this expression, the classical amplitude  $A = \left. \frac{\partial \theta'}{\partial p_\theta} \right|_{p'_\theta}$  is also evaluated at the stationary phase points  $(\theta_f, \theta_i)$ . The details of calculating the closed orbits and their properties that are required in this **primitive semiclassical  $S$ -matrix** are given in Appendix B.

Of course, all of the closed orbits that are used to construct  $\underline{S}^{\text{LR}}$  (5.39) depend both on the energy  $E$  of the electron, and external magnetic field  $B$  applied to the atom. In most cases, it is more useful to transform this  $S$ -matrix to the scaled variables  $(\epsilon, w)$  of Appendix A. Before giving the resulting scaled variable  $S$ -matrix, the issue of preconvolution must be addressed. When the semiclassical long-range  $S$ -matrix is used in the formula for the preconvolved cross section, Eq. (3.28), it is necessary to calculate

the  $S$ -matrix at complex energies  $E + i\Gamma/2$ . As discussed in Ch. 4 (see Eqs. (4.24-4.26)) when scaled variables are used, this translates into evaluating the long-range  $S$ -matrix at a complex value of the scaled field. That is, to preconvolve the cross section  $\sigma(w)$  or long-range  $S$ -matrix  $\underline{S}^{\text{LR}}(w)$  with a Lorentzian of width  $\Delta w$  in the  $w$  domain, the substitution

$$w \rightarrow w + i\frac{\Delta w}{2} \quad (5.40)$$

must be used in the scattering matrix  $\underline{S}^{\text{LR}}(w)$ . With this in mind, and using the relations  $S = w\tilde{S}$ ,  $r_0 = \tilde{r}_0(w/2\pi)^2$ , and  $p_\theta = \tilde{p}_\theta(2\pi/w)$  in Eq. (5.39), the preconvolved, scaled-variable  $S$ -matrix becomes:

$$\begin{aligned} S_{l'l',m}^{\text{LR}}(w) &= (2\pi)^{3/2}(-1)^{l+l'} \left(\frac{2\pi}{w}\right)^{1/2} \sum_{\text{c.o.}} \sqrt{|\tilde{A}| \sin \theta_i \sin \theta_f} Y_{lm}^*(\theta_f, 0) Y_{l'm}(\theta_i, 0) \\ &\times \exp\left(iw\tilde{S} - i\mu\frac{\pi}{2} + i\frac{3\pi}{4}\right) \exp\left(-\tilde{S}\frac{\Delta w}{2}\right). \end{aligned} \quad (5.41)$$

Note that the extra phase  $2\sqrt{8r_0}$  is simply the classical action from  $r_0$  to the origin and back again. Thus, in the scaled  $S$ -matrix (5.41) I have absorbed this phase into the scaled action of each orbit  $\tilde{S}$ . Because the closed classical orbits are completely independent of the scaled field  $w$ , the only effect of the complex value of the scaled field is to introduce a **damping factor**  $\exp(-\tilde{S}\Delta w/2)$  into the semiclassical  $S$ -matrix. This will have important consequences in the convergence of the semiclassical photoabsorption cross section developed in Ch. 6.

It is important to mention the conditions under which the semiclassical  $S$ -matrix, Eq. (5.39) or (5.41), is a good approximation. First, the derivation has assumed that the spherical harmonics vary slowly with the polar angles  $\theta$  and  $\theta'$  so that the stationary phase points are simply the radially launched and returning orbits. However, I emphasize that the effects of the nonradial trajectories are included approximately through the classical amplitude  $A$  of each orbit. Second, it is required that the stationary phase points (the radial orbits) exist, and are well isolated from each other. Lastly, although I have derived the long range  $S$ -matrix for an atom in an external magnetic field, the final result, Eq. (5.39), is also valid for an external electric field as well.

### 5.3 Special cases and improvements

In most cases, the semiclassical  $S$ -matrix derived in the previous section (5.39) provides an accurate description of the physics of an atomic electron in an external magnetic field. However, there are a number of situations in which this primitive semiclassical approximation fails. This section demonstrates how the ideas and tools of the previous section can be modified to treat these cases.

In general, one of the difficulties with semiclassical approximations is that when their primitive forms break down, a considerable amount of effort is required to repair them. This was first seen as researchers incorporated bifurcations [57] and continuous symmetries [133] into the semiclassical trace formula of Gutzwiller. The same has been true in semiclassical studies of atoms in external fields. As an example, since the original development of closed-orbit theory in 1988, only a few researchers [62, 54, 63] have attempted to give uniform semiclassical approximations for bifurcations of the closed orbits. Furthermore, because the standard formulation of closed-orbit theory uses semiclassical wavefunctions rather than Green's functions, many of the advances in the Green's function based trace formulas have not been applicable to closed-orbit theory. Thus, while uniform semiclassical approximations have been given for trace formulas, analogous progress in closed-orbit theory has lagged behind.

The approach of this chapter provides a simple solution to the difficulties found in improving the semiclassical approximations of closed orbit theory. In general, the semiclassical Green's function, Eq. (5.17), used to find the  $S$ -matrix is a very robust object. It is mainly when this configuration space Green's function is projected onto the channel functions (spherical harmonics) that difficulties arise. This section explores the long-range  $S$ -matrix for three cases where the above primitive version of the stationary phase technique given above fails. These instances are: the orbit parallel to the magnetic field, moderately high angular momentum elements of  $\underline{S}^{\text{LR}}$ , and bifurcations of the closed orbits. In each case, appropriately modified versions of the stationary phase technique give improved semiclassical  $S$ -matrices.

### 5.3.1 Parallel orbit

The most benign type of failure of Eq. (5.39) is when one of the angular factors in the  $S$ -matrix ( $\sin \theta$  or  $Y_{lm}(\theta, \phi)$ ) vanishes at the initial ( $\theta_i$ ) or final ( $\theta_f$ ) angle of the closed orbit. Then, the contribution of that orbit to the  $S$ -matrix will vanish unphysically. The most striking example of this is the closed orbit that is parallel to the magnetic field ( $\theta_i = \theta_f = 0$  or  $\pi$ ), for which the factor  $\sqrt{\sin \theta \sin \theta'}$  vanishes. A second example is the quasi-Landau orbit ( $\theta_i = \theta_f = \pi/2$ ), which gives a vanishing contribution to the  $S$ -matrix for odd parity states of the electron. The vanishing of these two orbits is known to be unphysical since both experiments and theory have seen their signatures in recurrence spectra. In both of these cases, the source of the error is in neglecting the angular dependences of factors such as  $\sin \theta$  or  $Y_{lm}(\theta, \phi)$  when the stationary phase integrals are done. Thus, the solution is to include, at least approximately, the strongest angular dependences of the Green's function in the stationary phase integrals.

This can be accomplished for the parallel orbit in a straightforward manner, beginning with the multidimensional Green's function, Eqs. (5.21) and (5.22), before the projection integrals over  $\theta$  and  $\theta'$  have been performed:

$$G_{lm,l'm'}(E) = \sum_{\text{traj}} \int d\theta d\theta' \Lambda_{ll'}^0(\theta, \theta') \sqrt{|A_1| \sin \theta \sin \theta'} e^{i(S(\theta, \theta') - \mu\pi/2)}, \quad (5.42)$$

$$\Lambda_{ll'}^0(\theta, \theta') = \frac{\sqrt{2\pi}}{r_0^2 |\dot{r}|} e^{-i(3\pi/4)} Y_{lm}^*(\theta, 0), Y_{l'm'}(\theta', 0). \quad (5.43)$$

Here, the factor  $\sqrt{\sin \theta \sin \theta'}$  has been placed explicitly in the Green's function, Eq. (5.42), rather than in the angular factor  $\Lambda_{ll'}^0(\theta, \theta')$ , Eq. (5.43), because its angular dependence must be included when the stationary phase integrals are performed. A superscript "0" is used on  $\Lambda_{ll'}$  in Eq. (5.43) to distinguish the factor for the parallel orbit  $\Lambda_{ll'}^0(\theta, \theta')$  (5.43) from that for the other orbits  $\Lambda_{ll'}(\theta, \theta')$ , Eq. (5.22). The only difference is that  $\Lambda_{ll'}^0(\theta, \theta')$  does not contain the factor  $\sqrt{\sin \theta \sin \theta'}$ . The following discussion will be presented for the parallel orbit having  $\theta_i = \theta_f = 0$ . However, the formulas also apply to the parallel orbit having  $\theta_i = \theta_f = \pi$ .

Because the main contribution of the projection integrals will come from the integrand's value

near  $\theta = \theta' = 0$ , small angle expansions of  $\sin \theta \approx \theta$  and  $\sin \theta' \approx \theta'$  can be used in Eq. (5.42):

$$G_{lm,l'm'}(E) \approx \int d\theta d\theta' \Lambda_{ll'}^0(\theta, \theta') \sqrt{|A_1|} \sqrt{\theta\theta'} e^{i(S(\theta, \theta') - \mu\pi/2)}. \quad (5.44)$$

Again, the remaining angular factor  $\Lambda_{ll'}^0(\theta, \theta')$  is assumed to vary slowly and will be evaluated at the stationary point of the integrand ( $\theta = \theta_f, \theta' = \theta_i$ ). From this point, the treatment of the integrals in Eq. (5.44) using stationary phase integration proceeds exactly as in the previous section. First, the integral over the initial angle  $\theta'$  is performed by expanding the action about the stationary phase point  $\theta' = \theta_i = 0$ . Again, the resulting stationary phase point is a classical orbit, the parallel orbit, that is launched radially along the direction of the magnetic field. A similar procedure is used for the final angle projection of Eq. (5.44). Both of these projections require the integral,

$$I_3(\alpha) = \int_0^\infty dx \sqrt{x} e^{\frac{i}{2}x^2\alpha} = \frac{1}{\sqrt{2}} e^{i3\pi/8} \Gamma\left(\frac{3}{4}\right) |\alpha|^{-3/4}, \quad (5.45)$$

where  $\Gamma(3/4) = 1.22541\dots$  is the the Gamma function. When the expansions of the action, Eqs. (5.23) and (5.31) are used along with the integral  $I_3$ , Eq. (5.45), to evaluate the integrals in Eq. (5.44), the resulting Green's function becomes,

$$G_{lm,l'm'}(E) \approx \frac{1}{2} \Lambda_{ll'}^0(\theta_i, \theta_f) \Gamma\left(\frac{3}{4}\right)^2 e^{i3\pi/4} \left| \frac{\partial p'_\theta}{\partial \theta'} \right|_{\theta}^{-3/4} \left| \frac{\partial p_\theta}{\partial \theta} \right|_{p'_\theta}^{-3/4} |A_1|^{1/2} e^{i(S - \mu\pi/2)}. \quad (5.46)$$

This formula applies to both orbits that move parallel to the external field ( $\theta_i = \theta_f = 0$  and  $\pi$ ) along the  $z$ -axis. The final form of the Green's function and  $S$ -matrix for these orbits is obtained by simplifying the combination of amplitudes in Eq. (5.46). This requires a careful handling of the partial derivatives:

$$\begin{aligned} \left| \frac{\partial p'_\theta}{\partial \theta'} \right|_{\theta}^{-3/4} \left| \frac{\partial p_\theta}{\partial \theta} \right|_{p'_\theta}^{-3/4} \left| \frac{\partial p'_\theta}{\partial \theta} \right|_{\theta'}^{1/2} &= \left| \frac{\partial(\theta', \theta)}{\partial(p'_\theta, \theta)} \right|^{3/4} \left| \frac{\partial(\theta, p'_\theta)}{\partial(p'_\theta, p_\theta)} \right|^{3/4} \left| \frac{\partial(p'_\theta, \theta')}{\partial(\theta, \theta')} \right|^{1/2} \\ &= \left| \frac{\partial(\theta, \theta')}{\partial(p'_\theta, p_\theta)} \right|^{3/4} \left| \frac{\partial(p'_\theta, \theta')}{\partial(\theta, \theta')} \right|^{1/2} \\ &= \left| \frac{\partial(\theta, \theta')}{\partial(p'_\theta, p_\theta)} \right|^{1/4} \left| \frac{\partial(p'_\theta, \theta')}{\partial(p'_\theta, p_\theta)} \right|^{1/2} \\ &= \left| \frac{\partial(\theta, \theta')}{\partial(p'_\theta, \theta')} \frac{\partial(p'_\theta, \theta')}{\partial(p'_\theta, p_\theta)} \right|^{1/4} \left| \frac{\partial(p'_\theta, \theta')}{\partial(p'_\theta, p_\theta)} \right|^{1/2} \\ &= \left| \frac{\partial(\theta, \theta')}{\partial(p'_\theta, \theta')} \right|^{1/4} \left| \frac{\partial(p'_\theta, \theta')}{\partial(p'_\theta, p_\theta)} \right|^{3/4} \\ &= \left| \frac{\partial \theta}{\partial p'_\theta} \right|_{\theta'}^{1/4} \left| \frac{\partial \theta'}{\partial p_\theta} \right|_{p'_\theta}^{3/4}. \end{aligned} \quad (5.47)$$

Furthermore, the first amplitude in this result  $\left| \frac{\partial \theta}{\partial p'_\theta} \right|_{\theta'}^{1/4}$  can be approximated as,

$$\begin{aligned} \left| \frac{\partial \theta}{\partial p'_\theta} \right|_{\theta'}^{1/4} &= \left| \frac{\partial p_\theta}{\partial \theta'} \right|_{\theta}^{-1/4} \\ &= \left| \frac{\partial p_\theta}{\partial \theta'} \Big|_{p'_\theta} + \frac{\partial \theta'}{\partial \theta} \Big|_{p_\theta} \frac{\partial p'_\theta}{\partial \theta'} \Big|_{\theta} \right|^{-1/4} \\ &\approx \left| \frac{\partial \theta'}{\partial p_\theta} \right|_{p'_\theta}^{1/4}. \end{aligned} \quad (5.48)$$

Combining Eqs. (5.47) and (5.48) for the amplitude, with Eq. (5.46) gives the final form of the semiclassical Green's function for the parallel orbit,

$$G_{lm,l'm'}(E) \approx \frac{1}{2} \Lambda_{ll'}^0(\theta_i, \theta_f) \Gamma \left( \frac{3}{4} \right)^2 e^{i3\pi/4} |A| e^{i(S-\mu\pi/2)}. \quad (5.49)$$

The manipulations of the classical amplitudes, Eqs. (5.47) and (5.48), are clearly the most difficult aspects of this derivation. In spite of that, the procedure for finding the semiclassical Green's function  $G_{lm,l'm'}(E)$  for the parallel orbits is straightforward: the integrals over  $\theta$  and  $\theta'$  are performed using the stationary phase technique, but including the angular dependence of the factor  $\sqrt{\sin \theta \sin \theta'} \approx \sqrt{\theta \theta'}$ .

The final long-range  $S$ -matrix for the parallel orbit is constructed using the Green's function (Eq. (5.49)), the angular factor  $\Lambda_{ll'}^0(\theta_i, \theta_f)$  (Eq. (5.43)), and the relationship between  $\underline{S}^{\text{LR}}$  and  $\underline{G}(r_0, r_0)$  (Eq. (5.10)):

$$S_{ll'}^{\text{LR}} = \sqrt{\frac{\pi}{2}} \Gamma \left( \frac{3}{4} \right)^2 (-1)^{l+l'} Y_{lm}^*(\theta_f, 0) Y_{l'm}(\theta_i, 0) |A| \exp \left( iS(\theta_f, \theta_i) + 2i\sqrt{8r_0} - i\mu \frac{\pi}{2} + i\pi \right). \quad (5.50)$$

The asymptotic, zero-energy Coulomb functions, Eq. (5.38), have been used in deriving this result. To rewrite this result in terms of scaled variables, the scaling relationships of Appendix A can again be used. In subsequent calculations, the scaled variable version of Eq. (5.50) will be used for the contribution of the parallel orbits, alongside Eq. (5.41) for the off-axis orbits. In both cases, the preconvolution of the  $S$ -matrix introduces the damping factor  $\exp(-\tilde{S}\Delta w/2)$  into the long-range  $S$ -matrix.

Note that the orbit parallel to the external field was first treated by Gao and Delos [51] using the semiclassical wavefunctions of closed-orbit theory. The approach given here has a similar form as their result, but exhibits a slightly different semiclassical amplitude  $A$ . The success of Eq. (5.50) will be seen

in next chapter (Ch. 6), where it is used to calculate the photoabsorption cross section of an atom in an external magnetic field. Also note that Eq. (5.50) is particularly relevant for an atom in an external electric field, where the dominant features in the recurrence spectrum are given by orbits parallel to the electric field.

### 5.3.2 High angular momentum

A second difficulty occurs for  $S$ -matrix elements  $S_{ll'}^{\text{LR}}$  having moderate and high values of the angular momenta  $l$  and  $l'$ . As described above, the stationary phase approximation leading to the  $S$ -matrices of Eqs. (5.39) and (5.50) assumes that the spherical harmonics vary slowly with the polar angles  $(\theta, \theta')$ . This approximation breaks down for high angular momentum where the spherical harmonics begin to oscillate rapidly.

For very high angular momenta, **all** of the angular dependence of the spherical harmonics can be included in the projection integrals (5.21). In this case, an improved stationary phase approximation leads to the modified stationary phase conditions  $p_\theta = \pm(l + 1/2)$  and  $p'_\theta = \pm(l' + 1/2)$ . In the limit  $l, l' \gg 1$ , these modified stationary phase conditions represent a correspondence principle (for  $p_\phi = 0$ ) between the quantum  $(l, l')$  and classical  $(p_\theta, p'_\theta)$  angular momentum. This approach is a straightforward generalization of the method of the previous section and includes nonradial trajectories explicitly in the final semiclassical  $S$ -matrix. In practice, this type of semiclassical approximation for the  $S$ -matrix  $\underline{S}^{\text{LR}}$  would be prohibitive because different  $S$ -matrix elements require a calculation of different classical trajectories. Moreover, it should not be necessary unless one is interested in treating initial electronic states with very high angular quantum numbers. For the low lying initial states of complex atoms, only moderate final state angular momenta are typically relevant. For these cases a simpler approximation is appropriate.

As the semiclassical approximation for the parallel orbit demonstrates, a simple way of improving the projection integrals of the Green's function is to include the lowest order variations of the offending angular factor. For moderate angular momentum  $S$ -matrix elements, this translates into expanding the spherical harmonics to linear order about the stationary phase points  $(\theta_i, \theta_f)$ . This approach is given here

and shows that the resulting correction to the primitive  $S$ -matrix (5.39) involves the derivatives of the spherical harmonics and powers of the classical amplitude  $A$ , Eq. (5.36), that appears in the primitive semiclassical approximation to  $\underline{S}^{\text{LR}}$ . Most importantly, the improved semiclassical  $S$ -matrix derived here still involves only radial launched and returning trajectories. Thus, the approximation circumvents the computational complications of searching for nonradial closed orbits.

The expansion of the spherical harmonics to linear order about the stationary phase points reads,

$$Y_{l'm}(\theta', 0) \approx Y_{l'm}(\theta_i, 0) + (\theta' - \theta_i) \left. \frac{\partial Y_{l'm}(\theta', 0)}{\partial \theta'} \right|_{\theta_i} \quad (5.51)$$

$$Y_{l'm}^*(\theta, 0) \approx Y_{l'm}^*(\theta_f, 0) + (\theta - \theta_f) \left. \frac{\partial Y_{l'm}^*(\theta, 0)}{\partial \theta} \right|_{\theta_f}. \quad (5.52)$$

The projection integral of the Green's function, Eqs. (5.21) and (5.22), can now be carried out using the stationary phase approach, but with one modification. Rather than performing the integrals over  $\theta$  and  $\theta'$  sequentially as before, both integrals are performed simultaneously. This leads to considerable simplifications and requires a two dimensional expansion of the classical action in the variables  $(\theta, \theta')$  about the stationary phase points  $(\theta' = \theta_i, \theta = \theta_f)$ . Defining the vector  $\vec{\alpha}$

$$\vec{\alpha} = \begin{pmatrix} \theta' - \theta_i \\ \theta - \theta_f \end{pmatrix}, \quad (5.53)$$

the two-dimensional Taylor series for the action reads,

$$S(\theta, \theta') = S(\theta_f, \theta_i) + \vec{\alpha}^\top \frac{\partial S}{\partial \vec{\alpha}} + \frac{1}{2} \vec{\alpha}^\top \frac{\partial^2 S}{\partial \vec{\alpha} \partial \vec{\alpha}} \vec{\alpha}, \quad (5.54)$$

where

$$\frac{\partial S}{\partial \vec{\alpha}} = \begin{pmatrix} \frac{\partial S}{\partial \theta'} \\ \frac{\partial S}{\partial \theta} \end{pmatrix} = \begin{pmatrix} -p_{\theta'} \\ p_\theta \end{pmatrix}, \quad (5.55)$$

$$\frac{\partial^2 S}{\partial \vec{\alpha} \partial \vec{\alpha}} = \begin{pmatrix} \frac{\partial^2 S}{\partial \theta' \partial \theta'} & \frac{\partial^2 S}{\partial \theta' \partial \theta} \\ \frac{\partial^2 S}{\partial \theta \partial \theta'} & \frac{\partial^2 S}{\partial \theta \partial \theta} \end{pmatrix}. \quad (5.56)$$

As before, the stationary phase condition  $(\frac{\partial S}{\partial \vec{\alpha}} = 0)$  selects radially traveling trajectories, the closed orbits, at small distances.

Next, the expansions of the action, Eq. (5.54), and of the spherical harmonics, Eqs. (5.51) and (5.52), are used in the yet to be projected Green's function, Eqs. (5.21) and (5.22). The term with the product  $Y_{lm}^*(\theta_f, 0)Y_{l'm}(\theta_i, 0)$  simply gives the result (5.39) of the previous section. The only nonvanishing correction term involves the derivatives of **both** of the spherical harmonics (if the angular dependence of  $\sqrt{\sin \theta \sin \theta'}$  is again neglected). After the slowly varying part of the integrand,

$$\sqrt{\sin \theta \sin \theta'} \left. \frac{\partial Y_{lm}^*(\theta, 0)}{\partial \theta} \right|_{\theta_f} \left. \frac{\partial Y_{l'm}(\theta', 0)}{\partial \theta'} \right|_{\theta_i}, \quad (5.57)$$

has been evaluated at the stationary phase points, the remaining integral can be performed:

$$I_2 = \int d\alpha_1 d\alpha_2 \alpha_1 \alpha_2 \exp\left(\frac{i}{2} \vec{\alpha} \cdot \frac{\partial^2 S}{\partial \vec{\alpha} \partial \vec{\alpha}} \cdot \vec{\alpha}\right) = -2\pi \left| \det \frac{\partial^2 S}{\partial \vec{\alpha} \partial \vec{\alpha}} \right|^{-1/2} \left. \frac{\partial \theta'}{\partial p_\theta} \right|_{p'_\theta} e^{-i\nu\pi/2}. \quad (5.58)$$

As before the index  $\nu$  counts the number of sign changes of the matrix  $\frac{\partial^2 S}{\partial \vec{\alpha} \partial \vec{\alpha}}$  along each trajectory. Using Eq. (5.58) and manipulating the classical amplitudes using Eq. (5.36), an expression for the corrected semiclassical Green's function (5.21) is found:

$$\begin{aligned} G_{l'l', m} &= (2\pi)^{3/2} i \sum_{traj} \frac{1}{r_0^2 |\dot{r}|} \sqrt{|A| \sin \theta_i \sin \theta_f} \\ &\times \left( Y_{lm}^*(\theta_f, 0) Y_{l'm'}(\theta_i, 0) + |A| e^{i\pi(\mu+1/2)} \frac{\partial Y_{lm}^*(\theta_f, 0)}{\partial \theta_f} \frac{\partial Y_{l'm}(\theta_i, 0)}{\partial \theta_i} \right) \\ &\times \exp\left(iS - i\mu \frac{\pi}{2} - i \frac{3\pi}{4}\right). \end{aligned} \quad (5.59)$$

The corresponding improved  $\underline{S}^{\text{LR}}$  from Eqs. (5.10) and (5.59), is then,

$$\begin{aligned} S_{l'l', m}^{\text{LR}} &= (2\pi)^{3/2} (-1)^{l+l'} \sum_{traj} \sqrt{|A| \sin \theta_i \sin \theta_f} \\ &\times \left( Y_{lm}^*(\theta_f, 0) Y_{l'm'}(\theta_i, 0) + |A| e^{i\pi(\mu+1/2)} \frac{\partial Y_{lm}^*(\theta_f, 0)}{\partial \theta_f} \frac{\partial Y_{l'm}(\theta_i, 0)}{\partial \theta_i} \right) \\ &\times \exp\left(iS + 2i\sqrt{8r_0} - i\sigma \frac{\pi}{2} + i \frac{3\pi}{4}\right). \end{aligned} \quad (5.60)$$

The sum over trajectories in these expressions is the same as in the primitive semiclassical long-range  $S$ -matrix: each classical trajectory that is launched radially outward from  $(r_0, \theta_i)$  and returns radially to  $(r_0, \theta_f)$  after accumulating a classical action  $S(\theta_f, \theta_i)$  contributes a term to the semiclassical  $S$ -matrix. In addition, the semiclassical amplitude  $A$  (5.36) and Maslov index  $\mu$  are the same as in the primitive semiclassical  $S$ -matrix, Eq. (5.39). Although this improved  $S$ -matrix, like traditional closed-orbit theory,

still involves only radial trajectories at  $r_0$ , it now includes the first-order corrections for higher angular momenta. In fact, by looking at the ratio

$$\eta = \left| \frac{Y_{lm}^*(\theta_f, 0) Y_{l'm'}(\theta_i, 0)}{A \frac{\partial Y_{lm}^*(\theta_f, 0)}{\partial \theta} \frac{\partial Y_{l'm'}(\theta_i, 0)}{\partial \theta'}} \right| \quad (5.61)$$

for each trajectory, the importance of the correction can be ascertained. Notice that when a trajectory lies near the node of a spherical harmonic, as in the above mentioned quasi-Landau orbit for odd parity states, the ‘‘correction’’ actually dominates the  $S$ -matrix. The original version of closed-orbit theory gives a vanishing recurrence strength for the odd parity quasi-Landau resonance. Shaw *et al.* [134] have given a similar correction for the quasi-Landau orbit as Eq. (5.60), but their result is only for the quasi-Landau orbit. The derivation presented here shows that such a correction term is present for all closed orbits when the angular momentum is moderate. However, most cases studied in this thesis have sufficiently low angular momentum that the correction derived here is unimportant except for the odd parity quasi-Landau recurrence.

### 5.3.3 Bifurcations

So far, corrections of the semiclassical  $S$ -matrix have been given for cases where the angle-dependent pieces, such as  $\sqrt{\sin \theta \sin \theta'}$  and  $Y_{lm}(\theta, \phi)$ , become important to include in the stationary phase integrals. The corrections given for the parallel orbit and for moderate angular momenta have made a common assumption: the stationary phase points exist and are well isolated from each other. It has been seen that the stationary phase points correspond to closed classical orbits. These orbits are launched radially outward from a sphere  $r = r_0$  in the matching region and return to the sphere radially after scattering classically off the long range fields. This radial trajectory approximation includes the effects of nonradial trajectories approximately through the classical amplitude  $A$  (5.36) in the semiclassical  $S$ -matrix. However, if a stationary phase point does not exist in the first place, the contributions of nearby nonradial orbits will be unrepresented in the long range  $S$ -matrix. This occurs near bifurcations of the closed orbits.

Bifurcations are a common feature of classically nonintegrable systems [109, 12]. For an atom

in a strong magnetic field, bifurcations of the closed orbits occur as the scaled energy  $\epsilon$  is increased [60]. Figure B.1 of Appendix B shows a map of the closed orbits for diamagnetic hydrogen. When the system is integrable ( $\epsilon = -\infty$ ) there is only one closed orbit, the familiar Kepler orbit in the Coulomb potential. As  $\epsilon$  increases, new orbits are born up until  $\epsilon = 0$  where there are infinitely many closed orbits. Delos and coworkers have used normal form theory [60, 61, 61] to analyze and study sequences of bifurcations of closed orbits in an external magnetic field. However, their analysis is purely classical. Only Main and Wunner [63] have attempted to include bifurcations of closed orbits in a semiclassical theory of photoabsorption. Their treatment uses semiclassical wavefunctions, alongside normal form theory, to construct uniform semiclassical approximations for a few types of bifurcations. It should be mentioned that this discussion applies only to the case of an external magnetic field; the bifurcations of closed orbits in external electric fields have been successfully included in a semiclassical formulation [62].

This final subsection sketches how bifurcations of closed orbits can be treated using the semiclassical approximations of this chapter. Because this work is still in progress, the emphasis will be on the qualitative features of the proposed approach rather than on formal derivations. In the language of this chapter, a bifurcation occurs when a new stationary phase point comes into existence at some scaled energy  $\epsilon_b$ . Thus, below the bifurcation point, the primitive semiclassical approximation for  $\underline{S}^{\text{LR}}$  shows no recurrence peak for the (nonexistent) closed orbit. Also, at the bifurcation point, the primitive semiclassical approximation, Eq. (5.39), diverges to infinity. That is, it shows an infinite recurrence strength. Of course, once the closed orbit has bifurcated, the  $S$ -matrices developed above are finite and give a good description of the associated recurrence peak. These predictions of the primitive semiclassical approximation are in disagreement with both experiment and accurate quantum calculations. First, below the classical bifurcation points small recurrence peaks are seen [44]. These prebifurcated orbits, ghost orbits, exist because the electron can tunnel into quantum mechanical paths that do not quite exist classically. Examples of these nonclassical paths were seen in the accurate quantum  $S$ -matrices of the previous chapter (Ch. 4). Second, quantum calculations and experiments alike show that the recurrence amplitudes are always finite at the bifurcation points. Thus, the divergence of closed-orbit theory, and the primitive semiclassical  $S$ -matrix of this chapter at the bifurcations is artificial.

A successful semiclassical theory of bifurcations, then, will include two features. First, the ghost orbits will be predicted. And second, the semiclassical amplitudes will be uniform (finite) as the scaled energy moves through the bifurcation point. The semiclassical theory of Main and Wunner [63] achieves both of these goals for certain types of bifurcations. However, their approach contains two difficulties. To extract the contributions of the prebifurcated ghost orbits, they analytically continue the classical trajectories into the complex plane. This substantially complicates numerical calculations of the closed orbits. When these complex ghost orbits are included into the semiclassical theory, their recurrence strength is seen to decay exponentially below the bifurcation point. However, an additional contribution below the bifurcation point is predicted that diverges exponentially. Main and Wunner handle this new divergence in the following manner [63]:

“In the above semiclassical formulas this complex-conjugate ghost would produce an unphysical exponential increase of the amplitude at energies below the bifurcation point. Thus we have as a by-product of the derivation of uniform semiclassical formulas that ghost orbits of this type have no physical meaning. In other words, they must not be included in the standard formulas since they do not appear in the asymptotic expansion of the uniform approximation ...”

In other words, certain predictions of their theory are discarded because they are unphysical. In spite of this, most aspects of Main and Wunner’s work appear to be well founded. This discussion shows, however, that the semiclassical theory for bifurcations of closed orbits in an external magnetic field is not completely understood.

I now give an outline of how bifurcations of closed orbits can be included in the semiclassical long-range  $S$ -matrix. The treatment begins with the Green’s function, Eq. (5.29), after the initial angle projection has been performed:

$$G_{lm,l'm'}(E) = \sqrt{2\pi i} \sum_{\text{traj}} \int d\theta \Lambda_{ll'}(\theta, \theta_i) \sqrt{|A_2(\theta, \theta_i)|} e^{i(S(\theta, \theta_i) - \mu(\pi/2))}. \quad (5.62)$$

In general, the amplitude in this formula,  $A_2 = \left. \frac{\partial \theta'}{\partial \theta} \right|_{p_\theta}$ , depends on the initial and final angles. The trajectories that contribute to this Green’s function are launched radially from a sphere in the matching region. However, when they return to the sphere, the trajectories have many different values of the classical angular momentum  $p_\theta$ . Next the main idea for treating bifurcations is presented.

Below a bifurcation point, there is simply no orbit that returns to the sphere radially. However, there are orbits that return to the sphere. As long as the sphere has a finite radius, well-behaved classical trajectories can be found that return to the sphere with nonzero angular momentum  $p_\theta$ . The reason that Main and Wunner have to calculate classical trajectories at complex energies is that they use a sphere having a vanishing radius  $r_0 = 0$ . Thus, below a bifurcation, no orbits (with real energies) reach their sphere and complex energy trajectories must be used instead. When closed orbits do exist, it is perfectly acceptable to launch trajectories from the origin. Because certain aspects of calculating closed orbits are simplified by this approach, many practitioners of closed-orbit theory have grown used to a sphere of zero radius. However, as Main and Wunner's work shows, insisting upon using a sphere of zero radius leads to considerable complications when radially launched and returning closed orbits do not exist. I emphasize, however, that when trajectories are launched from a finite sphere, the ghost orbits can be understood as simply being related to classical orbits that return to the sphere nonradially.

Figure 5.1 shows an example of the nonradial ghost orbits for scaled energies near the saddle-node bifurcation of the  $X_1$  exotic orbit (see Fig. B.1). Below the bifurcation energy ( $\epsilon_b = -0.115$ ) nonradial orbits are seen to return to the sphere of scaled radius  $\tilde{r}_0 = 0.1$ . To include nonradial orbits, such as those shown in Fig. 5.1, into the semiclassical  $S$ -matrix, two steps are required. First, the graph of the classical action as a function of the final angle is fit to a polynomial form. For example, the classical actions shown in Fig. 5.1 can be approximated by the polynomial:

$$\tilde{S}(\theta_f, \tilde{p}_{\theta_i} = 0) = \tilde{S}(\theta'_f) + (\theta_f - \theta'_f)a(\epsilon) + \frac{1}{2}(\theta_f - \theta'_f)^2b(\epsilon). \quad (5.63)$$

The expansion point  $\theta'_f$  used in this approximation is chosen to be the leftmost point of the family of orbits that return to the sphere. The fit parameters  $a(\epsilon)$  and  $b(\epsilon)$  are functions of the scaled energy, with the most important dependence being contained in  $a(\epsilon)$ ; as  $a(\epsilon)$  crosses through zero from below, the new closed orbits bifurcate. Each type of bifurcation will have a different polynomial associated with it [135]. Once the fit of the action, Eq. (5.63), has been found for the bifurcation being studied, it is used in the Green's function, Eq. (5.62), when the final angle projection integral is performed. In general, the angular dependence of the amplitude  $A_2$  must also be taken into account. Although the

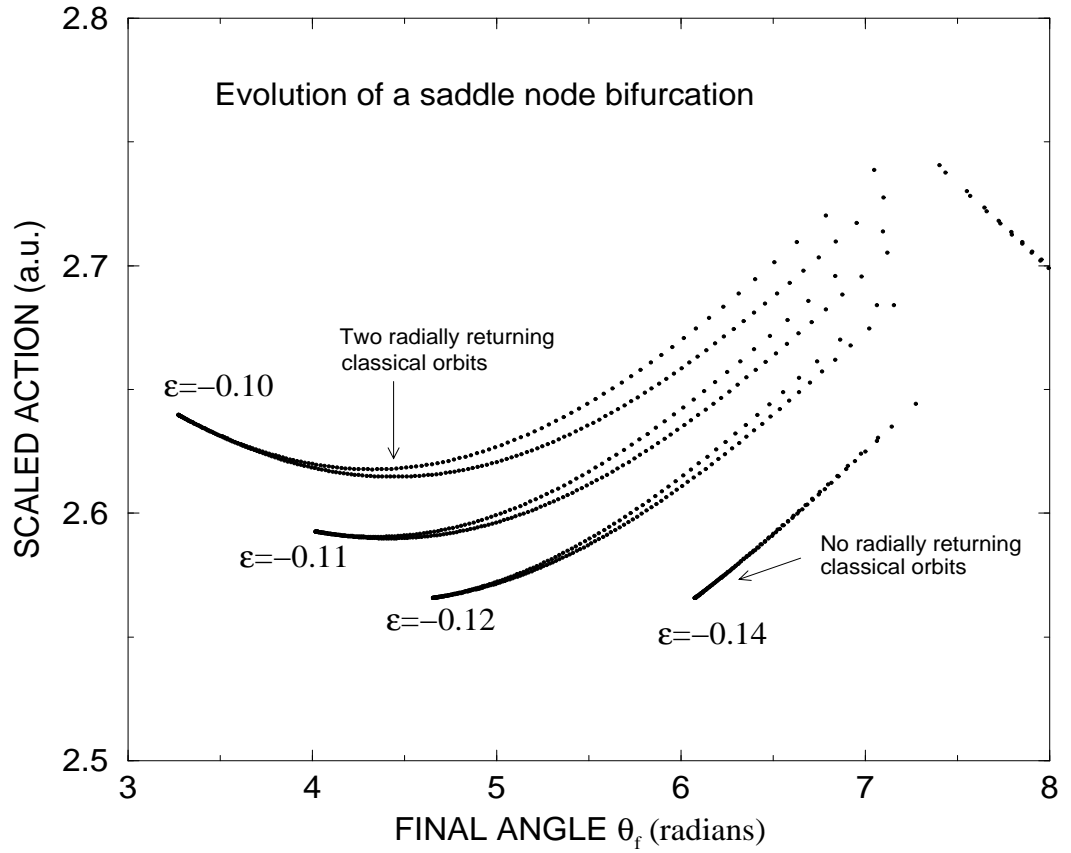


Figure 5.1: The classical scaled action  $\tilde{S}(\theta_f)$  is given as a function of the final angle  $\theta_f$  for trajectories returning to a sphere of scaled radius  $\tilde{r}_0 = 0.1$ . The trajectories were launched radially outward from the same sphere. At the lower two scaled energies ( $\epsilon = -0.14, -0.12$ ) there is no radially returning orbit (remember that  $\tilde{p}_\theta$  is simply the slope of the scaled action in this graph). At a scaled energy of  $\epsilon = -0.115$ , a pair of exotic orbits ( $X_{1a}, X_{1b}$ ) bifurcates. These newly existing closed orbits appear as the local minima in the scaled actions at the upper two scaled energies ( $\epsilon = -0.11, -0.10$ ). Most importantly, below the bifurcation energy, nonradial classical trajectories are seen to reach the final sphere.

resulting integrals are typically more complicated than the simple Gaussian forms found in the primitive semiclassical  $S$ -matrix, they can often be performed analytically. By carrying out these steps, a uniform semiclassical theory for long-range  $S$ -matrix can be derived.

The details of this approach depend strongly on the particular form of the action near the bifurcation. A general study needs to be carried out of the normal forms of the actions near different types of bifurcations. Although Main and Wunner have given such expressions for some types of bifurcations, they use a variable other than the final angle in which to expand the action. It would be useful to transform their normal forms to the final angle representation used here. Many of the details in treating bifurcations still need to be investigated. However, the approach described here provides a beginning point for future investigations. Again, the main advantage of this method is that the classical trajectories do not need to be calculated at complex energies.

## 5.4 Results

In this chapter, I have developed semiclassical approximations for the long-range  $S$ -matrix  $\underline{S}^{\text{LR}}$ . After the primitive semiclassical approximation to  $\underline{S}^{\text{LR}}$  was derived, extensions of the basic method were given for a number of special cases. The main use of the semiclassical scattering matrices of this chapter is to enable a semiclassical approximation for the photoabsorption cross section. This development will be presented in the following chapter (Ch. 6). However, before moving on, it is useful to compare the semiclassical long-range  $S$ -matrix, with the accurate quantum  $S$ -matrices of the previous chapter (Ch. 4).

Figures 5.2 and 5.3 show such a comparison at a scaled energy of  $\epsilon = -0.3$ , where the classical dynamics are mostly chaotic. Again, the comparison is performed by studying the recurrences in the matrix elements of  $\underline{S}^{\text{LR}}$ . Reasonably good quantitative agreement is seen between the semiclassical and quantum results. The main discrepancies are the nonclassical ghost orbits, labeled with the letter “g”, which appear in the quantum recurrence strengths but are absent from the semiclassical. The improved semiclassical formulas for moderate angular momentum and the parallel orbit have been used to obtain these results.

With all of the necessary tools in hand, semiclassical approximations to the photoabsorption cross

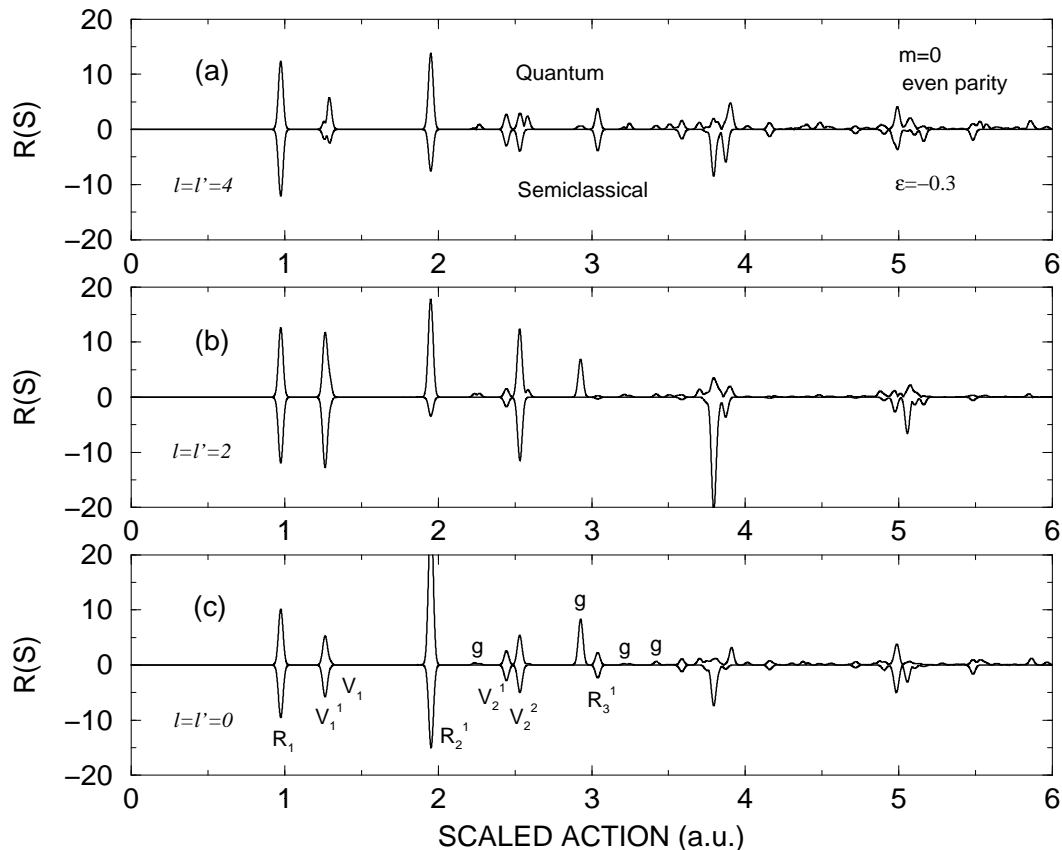


Figure 5.2: A comparison is shown between the quantum (upright) and semiclassical (inverted) recurrence strengths  $R(\tilde{S})$  of elements of  $\underline{S}^{\text{LR}}$ . More specifically, the recurrence strengths Eq. (4.27), of  $Re(S_{00}^{\text{LR}}(w))$  (c),  $Re(S_{22}^{\text{LR}}(w))$  (b) and  $Re(S_{44}^{\text{LR}}(w))$  (a), are shown for  $m = 0$ , even parity states of diamagnetic hydrogen at a scaled energy of  $\epsilon = -0.3$ . The semiclassical  $S$ -matrix has been calculated using the formulas derived in this chapter, Eqs. (5.41) and (5.50). The 26 closed orbits contributing to the semiclassical  $S$ -matrix have been calculated numerically. The detailed properties of these closed orbits, including the labeling scheme used here, can be found in Appendix. B. The accurate quantum  $S$ -matrix elements were calculated with the variational  $R$ -matrix method described in Ch. 4 using a preconvolution smoothing width of  $\Delta w = 0.4$ . The semiclassical  $S$ -matrix has also been preconconvolved with the same width. Some of the shorter action closed orbits have been labeled ( $R_1, V_1^1, V_1, \dots$ ) as have the ghost orbits ( $g$ ) in the quantum recurrence strengths that correspond to no classical closed orbit. The Fourier transform was carried out over the range of  $w$  from 100 to 500.

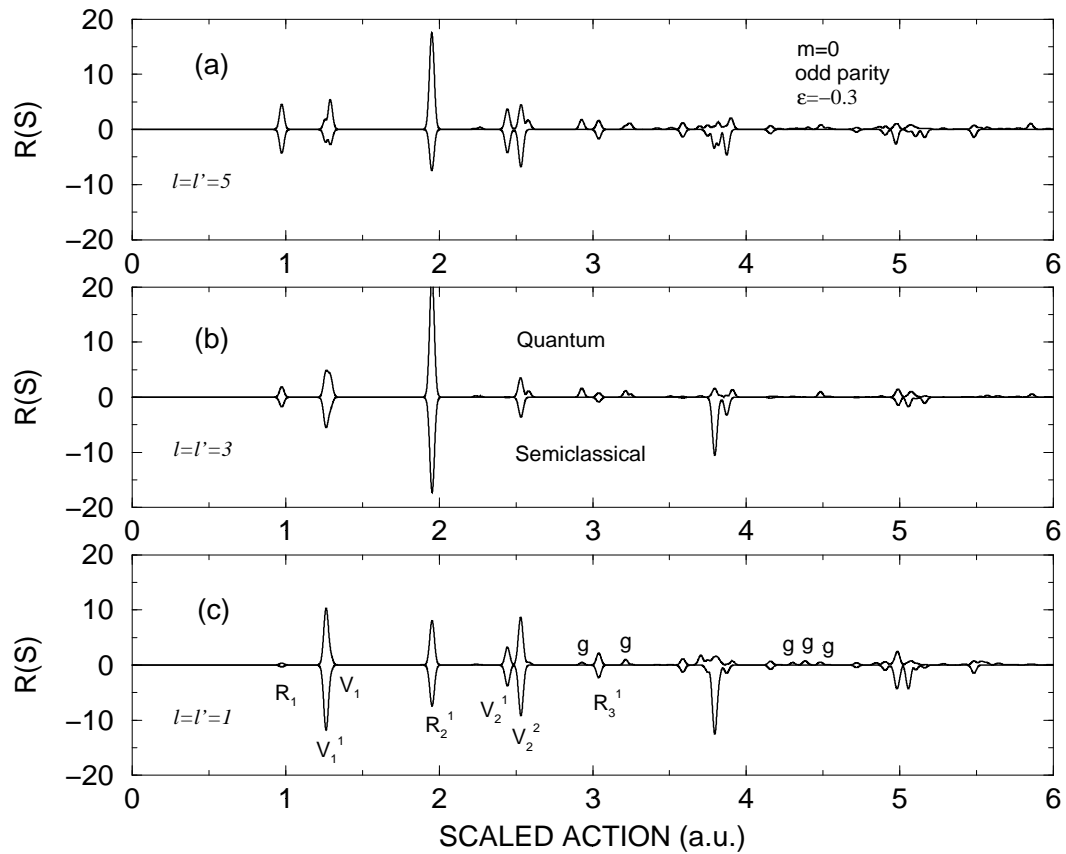


Figure 5.3: A comparison is shown of quantum (upright) and semiclassical (inverted) recurrence strengths for odd parity,  $m = 0$ , elements of the long-range  $S$ -matrix. The Fourier transforms, Eq. (4.27), of the semiclassical and quantum  $S$ -matrix elements  $Re(S_{11}^{LR}(w))$  (c),  $Re(S_{33}^{LR}(w))$  (b) and  $Re(S_{55}^{LR}(w))$  (a) shown here were calculated in the same manner as in the even parity case presented in Fig. 5.2. The smoothing width used here is slightly larger,  $\Delta w = 0.6$ . However, the scaled energy  $\epsilon = -0.3$  and range of  $w$  values used (100 – 500) are the same as in Fig. 5.2. Thus, the same set of closed orbits used for the even parity case also contribute to the recurrence strengths here; only the amplitudes are changed for the different angular momenta. The success of the semiclassical approximation for moderate angular momentum, Eq. (5.60), is seen in the accurate prediction of the odd parity quasi-Landau recurrence peak  $R_1$ . The primitive semiclassical approximation gives a vanishing contribution of this orbit because the odd parity spherical harmonics have a node at  $\theta_i = \theta_f = \pi/2$ .

section can now be studied.